NASA TM-85694

NASA Technical Memorandum 85694

NASA-TM-85694 19830028239

A FRACTURE MECHANICS APPROACH FOR DESIGNING ADHESIVELY BONDED JOINTS

W. S. Johnson and S. Mall

September 1983

NASA
National Aeronautics and
Space Administration

Langley Research Center
Hampton, Virginia 23665

A FRACTURE MECHANICS APPROACH FOR DESIGNING ADHESIVELY BONDED JOINTS

W. S. Johnson and S. Mall*

SUMMARY

An analytical and experimental investigation was undertaken to determine if the adhesive debond initiation stress could be predicted for arbitrary joint geometries. The analysis was based upon a threshold total strain-energy-release rate (G_{th}) concept. Two bonded systems were tested: T300/5208 graphite/epoxy adherends bonded with either EC-3445 or FM-300 adhesive. The G_{th} for each adhesive was determined from cracked-lap-shear (CLS) specimens by debond initiation tests. Finite-element analyses of various tapered CLS specimen geometries predicted the specimen stress at which the total strain-energy-release rate (G_T) equaled G_{th} at the joint tip. Experiments verified the predictions. The approach described herein predicts the maximum stress at which an adhesive joint can be cycled yet not debond. Furthermore, total strain-energy-release rate appeared to be the driving parameter for cyclic debonding and debond initiation in structural adhesives. In addition, debond initiation and growth were found to occur with virtually no peel stress present.

---

*Associate Professor, University of Maine, working under NASA Cooperative Agreement NCC1-70.

SYMBOLS LIST

a	length of debond, m
$\frac{da}{dN}$	debond growth rate, m/cycle
C,n	curve-fit parameters
E	Young's modulus of composite, Pa
E_1,E_2	Young's moduli of composite, Pa
G	shear modulus of adhesive, Pa
G_{12}	shear modulus of composite, Pa
G_I	mode I strain-energy-release rate, J/m^2
G_{II}	mode II strain-energy-release rate, J/m^2
G_T	total strain-energy-release rate ($= G_I + G_{II}$), J/m^2
G_{th}	threshold total strain-energy-release rate, J/m^2
N	number of cycles
P	applied load, N
R	stress ratio, minimum stress/maximum stress
r	residual from least-square curve fit
S_{th}	predicted maximum stress level in strap adherent without debond initiation or growth, Pa
α	taper angle of lap adherend, degrees
ν	Poisson's ratio of adhesive
ν_{12},ν_{23}	Poisson's ratios of composite

INTRODUCTION

One major obstacle to optimizing composite structures is the strength and fatigue penalty introduced by mechanical fasteners at joints. Mechanical fastener holes may degrade static strength by as much as 50 percent. Adhesively bonded joints are a viable alternative to mechanical fastening. Currently, most aerospace companies are reluctant to use adhesive bonding to join primary aircraft structure. This reluctance is due, in part, to the lack of understanding of the adhesive bond behavior, and reliable and efficient design procedures. The objective of this paper is to present an analytical design approach, based on fracture mechanics, for adhesively bonded joints.

Previous work by the authors [1] has shown a correlation between total strain-energy-release rate (G_T) and debond propagation rate (da/dN). Herein, data were gathered from cracked-lap-shear specimens that had quasi-isotropic graphite/epoxy (T300/5208)* composite adherends. Two adhesives were tested: FM-300* and EC-3445*. The strain-energy-release rates (G_T, G_I, and G_{II}) at the debond tips were calculated using the GAMNAS [2] finite-element program. The previous study [1] found that G_T correlated the debond growth rate better than either G_I or G_{II} did. The G_T versus da/dN data are plotted in Fig. 1 for the FM-300 and EC-3445. On these log-log plots, the data are represented very well by a straight line given by the following equation:

$$\frac{da}{dN} = C(G_T)^n \tag{1}$$

where n is the slope of the line in the plot. The values of n found in the previous investigation ranged from 4 to 4.5. These values are quite high

*The use of trade names in this paper does not constitute endorsement, either expressed or implied, by the National Aeronautics and Space Administration.

when compared with typical values of n derived from applying Eq. (1) to fatigue crack growth in aluminum and steel alloys, where n ranges from 1.5 to 3 [3]. Steep slopes mean that small changes in applied load cause a large change in debond growth rate. Thus, the debond propagation rate in adhesive joints is more sensitive to errors in design loads than is typical crack growth rate in metallic structures. Because of this sensitivity, the design of bonded joints for finite life may be difficult. Minor design alterations or small analysis errors could cause large changes in actual and predicted lives. A viable alternative design procedure would be an infinite-life approach. The no-growth threshold, G_{th}, may be an important material property for bonded systems. The premise for this research paper is as follows:

> Given that the value of G_{th} has been correctly defined and found experimentally for a given adhesive, one should be able to predict the threshold (i.e., no debond growth) stress for arbitrary joint geometries using the same adhesive system.

The following sections will describe the test specimens, analysis, and experimental procedures used to verify this premise.

EXPERIMENTS

Test Specimen

The cracked-lap-shear (CLS) specimen, shown in Fig. 2, was employed in the previous study [1] because it represents a simple structural joint subjected to in-plane loading. Both shear and peel stresses are present in the bond line of this joint. The magnitude of each component of this mixed-mode loading can be modified by changing the relative thicknesses of strap and lap adherends [2,4].

The present study used the same cracked-lap-shear specimen design described above, except that many of the lap adherends were machined to tapers, as shown in Fig. 3. Specimens with taper angles of 5°, 10°, 30°, and 90° (untapered) were tested. Different tapers gave different values of G_I, G_{II}, and G_T for the same applied load. This will be discussed further in a later section.

Two bonded systems were studied: graphite/epoxy (T300/5208) adherends bonded with either EC-3445 adhesive or with FM-300 adhesive. The EC-3445 adhesive is a thermosetting paste with a cure temperature of 121°C; specimens were fabricated by conventional secondary bonding procedures. On the other hand, the FM-300 is a modified epoxy adhesive supported with a carrier cloth with a cure temperature of 177°C; specimens were fabricated by co-cure, whereby adherends were cured and bonded simultaneously. The bonding processes followed the manufacturers' recommended procedures for each adhesive. The nominal adhesive thickness was 0.10 and 0.25 mm for the EC-3445 and FM-300, respectively. These adhesives and adherends are also being employed in an Army program to build an all-composite helicopter airframe that is almost entirely adhesively bonded [5].

The Young's modulus of FM-300 adhesive was calculated from the shear modulus provided by the manufacturer, assuming the adhesive to be an isotropic material. The EC-3445 adhesive is the paste version of the AF-55 adhesive film; therefore, the Young's modulus of EC-3445 was calculated from the shear modulus of AF-55 [6] by assuming the adhesive to be an isotropic material. Poisson's ratio was assumed to be 0.4 for both adhesives, which is a typical value for adhesives. The material properties of each adhesive are given in Table 1.

The composite adherends consisted of quasi-isotropic layups of $[0/45/-45/90]_S$ and $[0/45/-45/90]_{2S}$. The material properties of

graphite/epoxy, presented in Table 2, were obtained from Ref. 7. For each bonded system, two types of specimen were tested: (1) thin lap adherend of 8 plies bonded to thick strap adherend of 16 plies, and (2) thick lap adherend of 16 plies bonded to thin strap adherend of 8 plies. These geometries and number of specimens tested are listed in Table 3.

Testing Procedure

The test program was conducted to establish the minimum applied cyclic stress in the strap adherend that would cause debond initiation and growth in the adhesive bond line of the tapered cracked-lap-shear specimen. To this end, virgin specimens (no debonds) were tested at a given load range for 1-million cycles, then inspected using dye-enhanced (zinc iodide) radiography. The cyclic stress ratio, R, was 0.1 and the cyclic frequency was 10 Hz. If there was evidence of debond initiation, the test was stopped. Otherwise, the cyclic load level was raised by approximately 10 percent, keeping $R = 0.1$. The specimen was tested for an additional 1-million cycles and then radiographed. These steps were repeated, progressively increasing the load range until the specimen showed signs of debonding. This procedure allowed for more data points to be obtained per specimen.

Several tests were run on virgin specimens to verify that the increasing load did not influence the results. The virgin specimens debonded at stress levels at or very near the one found by the progressive technique. Thus, the prior low-level cycling was assumed to have no significant effect on the specimen.

After a fatigue-induced debond was found, the specimen was removed from the test machine. In many cases, the specimen was remachined to another lap adherend taper and retested. The tip of the new taper was always at least 8 mm from the previous debond tip.

ANALYTICAL PREDICTION OF DEBOND THRESHOLD STRESSES

Finite-Element Analysis

The cracked-lap-shear specimens were analyzed with the finite-element program GAMNAS [2] to determine the strain-energy-release rate for given geometry, debond length, and applied load. This two-dimensional analysis accounts for the geometric nonlinearity associated with the large rotations in the unsymmetric cracked-lap specimen.

A typical finite-element model (FEM) of a tapered cracked-lap-shear specimen (with 10° taper) is shown in Fig. 4. This FEM mesh consisted of about 1200 isoparametric 4-node elements and had about 2400 degrees of freedom. Each ply of composite was modeled as a separate layer in the finite-element model, except for the ply at the adhesive interface which was modeled in two or three layers. The adhesive was modeled with four layers of elements. A multipoint constraint was applied to the loaded end of the model to prevent rotation (i.e., all of the axial displacements along the ends are equal to simulate actual grip loading of the specimen). Plane-strain conditions were assumed in the finite-element analysis. The material properties of composite adherends and adhesives are listed in Tables 1 and 2. The strain-energy-release rate was computed using a virtual crack-closure technique. The details of this procedure are given in Ref. 8.

The previous study [1] indicated that at least 12 elements were required through the adhesive thickness to reach convergence on G_I and G_{II} calculations. However, the calculation of G_T was not affected by the number of elements through the adhesive thickness. Since the previous study indicated that G_T correlated the da/dN just as well (and perhaps better) than either G_I or G_{II} separately, the authors have chosen to base their design criterion on G_T. Thus, four elements through the adhesive thickness were considered more than sufficient to calculate G_T.

Debond Threshold Predictions

The premise that a material property, G_{th}, could be determined and used to predict debond threshold stresses in arbitrary joint geometries was verified in the current study by the following procedure.

1. The minimum cyclic load that initiated debonds in tests of the untapered-adherend ($\alpha = 90°$) specimens was used in the GAMNAS program to calculate G_T. This G_T was taken to be equal to G_{th}.
2. For each of the tapered-adherend geometries, the GAMNAS program was used to calculate the stress required in the strap adherend to create a value of G_T equal to G_{th}.
3. The minimum cyclic stresses required to initiate debonds in tests of the tapered-adherend specimens were compared to the predicted stresses.

To compute a debond threshold stress, a small debond must be assumed to exist at the location of expected debond initiation, that is, at the end of the strap adherend. For the current computations, a debond length of 1 mm was assumed. This debond length was typical of the lengths found by the X-ray inspection technique during the debond initiation tests. Computations using a debond length of 0.5 mm resulted in predicted initiation stresses about 3 percent lower than those for a 1 mm length.

In addition to G_T, a rough estimate of the G_I/G_{II} ratio was calculated for each specimen type. All analytical results are presented in Table 3.

RESULTS AND DISCUSSION

The minimum cyclic stresses that initiated debonds in the tests of the tapered-adherend specimens and the analytical predictions of those stresses are plotted in Fig. 5. The solid symbols in the figure represent specimens that initiated and grew debonds within 1-million cycles. The open symbols represent specimens that were cycled to at least 1-million cycles and no

debonding was evident from the radiographs. The lines in the figure are the predicted debond threshold stresses as a function of taper angle presented in Table 3.

The data show a significant improvement in debond resistance for taper angles below 10°. The 5° taper results in a threshold stress level about 50 percent higher than that for no taper (α = 90°). Figure 5 also shows clearly that joints fabricated with FM-300 adhesive can be subjected to 50 percent higher loads than EC-3445 without debonding. The relative difference between the two adhesives would probably vary with test environment.

The predicted debond initiation threshold stresses are in excellent agreement with the experimental data for each adhesive for the specimen geometries studied. These results are particularly revealing in that threshold values based on total strain-energy-release rate predicted the test results so well. At a 90° taper, the G_I/G_{II} ratio is approximately 0.20 and 0.26 for EC-3445 and FM-300 adhesives, respectively. For the 5° and 10° tapers, the G_I/G_{II} ratio is practically zero for both adhesives. According to Hart-Smith [9], a 5° taper should eliminate all of the peel stresses and the specimen should not debond. This study indicates that a 5° taper does indeed eliminate peel stresses for all practical purposes, but the taper hardly guarantees that no debonding will occur. Clearly, G_I alone cannot be used to explain the trend of the data in Fig. 5.

The debond initiation tests resulted in a G_{th} very close to the G_T associated with a debond propagation rate of 10^{-6} mm/cycle (3.94×10^{-8} in./cycle). The authors feel that 10^{-6} mm/cycle is a sufficiently low crack growth rate upon which to base a threshold value -- particularly if G_{th} is taken on the conservative side of the data, as shown in Fig. 1. The two approaches ($da/dN = 10^{-6}$ mm/cycle and debond initiation) agreed closely

despite the absence of a clear "knee" in the da/dN vs. G data commonly associated with threshold. However, before a clear correlation between debond initiation and the crack growth threshold can be established, more crack growth rate data are needed at very low rates to see if a "knee" really exists.

Total strain-energy-release rate, G_T, appears to be the driving factor for debonding of these rather tough structural adhesives (EC-3445 and FM-300). O'Brien [10] has found G_T to be the driver for cyclic delamination growth in polymer matrix composites. Liechti and Knauss [11] have also suggested, for adhesive joints, that G_T may the the driver for debond extension based on observations of a polyurethane elastomer.

DESIGN APPROACH

The proposed design technique can be applied to actual structures as follows. First, from basic laboratory coupons, such as the untapered (i.e., $\alpha = 90°$) CLS specimen, tested in the usage environment (e.g., temperature, humidity, and cyclic frequency), the G_{th} value for the adhesive system of interest can be determined. This, of course, requires a proper analysis of the specimen to determine G_T.

Second, an initial flaw (debond) size must be assumed. This would normally be either (1) the largest size debond due to manufacture that might not be found during inspection or (2) the largest debond that might result from operational damage.

Finally, a proposed structural joint geometry can be sized to insure no debonding. This requires an iterative process by which the geometry and loading are analyzed to insure that G_T at the assumed debond tip is less than or equal to G_{th}.

CONCLUSIONS

An analytical approach for predicting the maximum cyclic stress that an adhesive joint can sustain without debonding has been presented and verified. This approach, based on fracture mechanics, depends on the experimental determination of a total strain-energy-release rate threshold value. The analytical predictions were verified by experimental data generated on graphite/epoxy adherends bonded with either FM-300 or EC-3445 adhesives. The following conclusions were obtained:

1. Analytical predictions of the loads required to initiate debonds in tapered adherend CLS specimens agreed well with experimental results.
2. Total strain-energy-release rate, G_T, appears to be the governing parameter for cyclic debonding and debond initiation in tough structural adhesives.
3. Debond initiation and growth can occur in the absence of peel stresses.
4. FM-300 adhesive exhibited superior debond resistance compared to EC-3445 adhesive.
5. Changing the taper of the lap adherend from 90° to 5° increased the no-growth threshold nondamaging stress range by almost 50 percent.

REFERENCES

[1] Mall, S., Johnson, W. S., and Everett, R. A., Jr., "Cyclic Debonding of Adhesively Bonded Composites," NASA TM-84577, Washington, DC, Nov. 1982.

[2] Dattaguru, B., Everett, R. A., Jr., Whitcomb, J. D., and Johnson, W. S., "Geometrically-Nonlinear Analysis of Adhesively Bonded Joints," NASA TM-84562, Washington, DC, Sept. 1982.

[3] Damage Tolerant Design Handbook, Battelle Metals and Ceramics Information Center, Columbus, OH, 1972.

[4] Brussat, T. R., Chiu, S. T., and Mostovoy, S., "Fracture Mechanics for Structural Adhesive Bonds," AFML-TR-163, Air Force Materials Laboratory, Dayton, OH, 1977.

[5] Alsmiller, G. R., Jr. and Anderson, W. P., "Advanced Composites Airframe Program - Preliminary Design," USAAVRADCOM-TR-80-D-37A, U.S. Army Aviation Research and Development Command, 1982.

[6] Hughes, E. J. and Rutherford, J. L., "Evaluation of Adhesives for Fuselage Bonding," Report No. KD-75-74, The Singer Company, 1975.

[7] Shivakumar, K. N. and Crews, J. H., Jr., "Bolt Clampup Relaxation in a Graphite/Epoxy Laminate," NASA TM-83268, Washington, DC, 1982.

[8] Rybicki, E. F. and Kanninen, M. F., "A Finite Element Calculation of Stress Intensity Factors by a Modified Crack Closure Integral," Engineering Fracture Mechanics, Vol. 9, No. 4, 1977, pp. 931-938.

[9] Hart-Smith, L. J. and Bunin, B. L., "Selection of Taper Angles for Doubles, Splices, and Thickness Transition in Fibrous Composite Structures," Douglas Paper 7299, McDonnell Douglas Corporation, 1983. (Presented at Sixth Conference on Fibrous Composites in Structural Design, New Orleans, LA, Jan. 24-27, 1983.)

[10] O'Brien, T. K., "Mixed-Mode Strain-Energy-Release Rate Effects on Edge Delamination of Composites," NASA TM-84592, Washington, DC, Jan. 1983.

[11] Liechti, K. M. and Knauss, W. G., "Crack Propagation at Material Interfaces: II Experiments on Mode Interaction," Experimental Mechanics, Vol. 22, No. 10, Oct. 1982, pp. 383-391.

Table 1--Adhesive material properties.

	Modulus, GPa		Poisson's Ratio
	E	G	ν
EC-3445 (3M Company)	1.81	0.65	0.4
FM-300 (American Cyanamid Company)	2.32	0.83	0.4

Table 2--Graphite/epoxy[a] adherend material properties.

Modulus,[b] GPa			Poisson's Ratio[b]	
E_1	E_2	G_{12}	ν_{12}	ν_{23}
131.0	13.0	6.4	0.34	0.34

[a]T300/5208 (NARMCO), fiber volume fraction is 0.63.

[b]The subscripts 1, 2, and 3 correspond to the longitudinal, transverse, and thickness directions, respectively, of a unidirectional ply.

Table 3--Tapered CLS specimens.

Adhesive	Taper Angle, $\alpha°$	Plies Strap / Plies Lap	Number of Test Specimens	Analytical Results S_{th}, MPa	Analytical Results G_I/G_{II}*
EC-3445 G_{th} = 38 J/M^2	5	8/16	3	120	0
	10	16/8	3	102	0
	30	16/8	4	88	.18
	90	8/16	4	80	.20
FM-300 G_{th} = 87 J/m^2	5	16/8	3	164	0
	10	16/8	4	149	0
	30	16/8	4	130	.22
	90	16/8	3	121	.26

*Approximate ratio. Mesh was not fine enough for convergence. Four elements through the adhesive thickness.

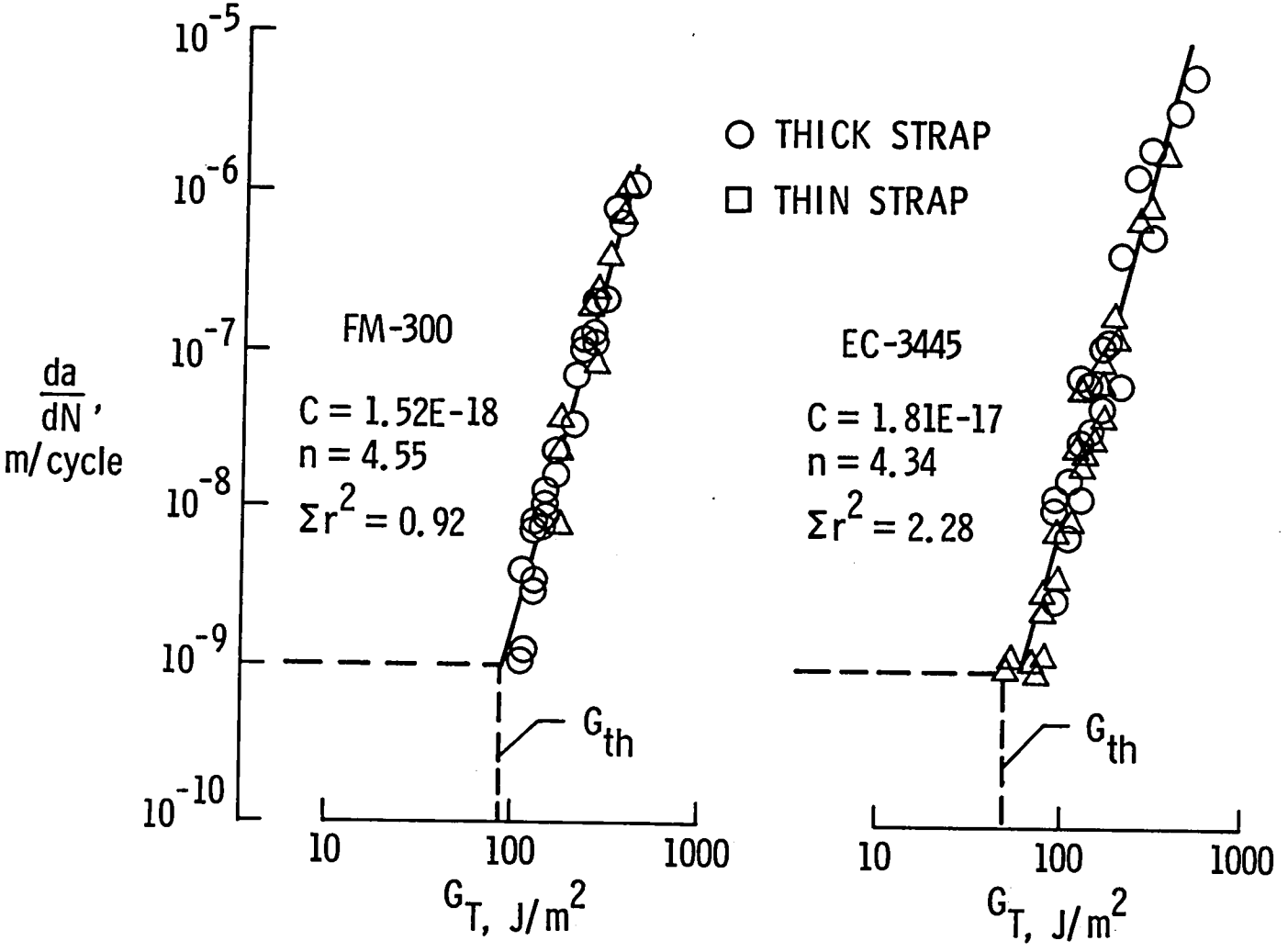

Figure 1.- Relation between total strain-energy-release rate and debond growth rate for both FM-300 and EC-3443 adhesive (ref. 1).

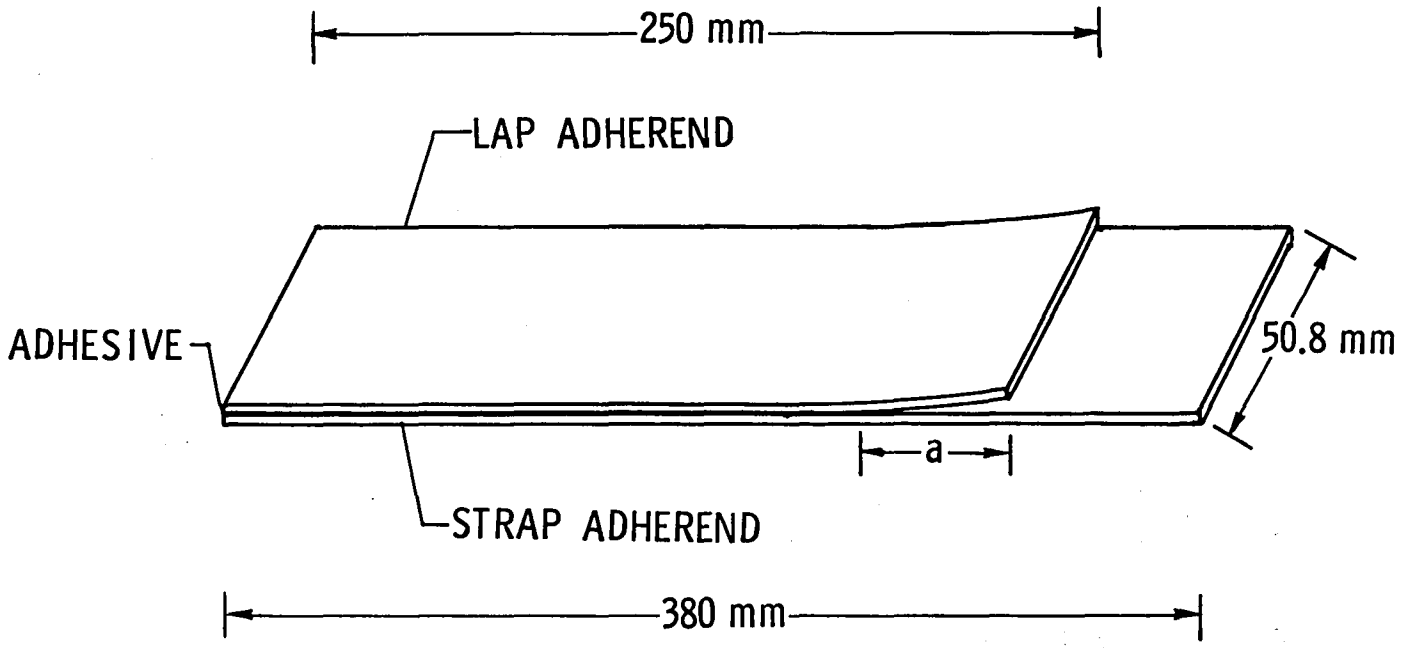

Figure 2.- Cracked-lap-shear specimen.

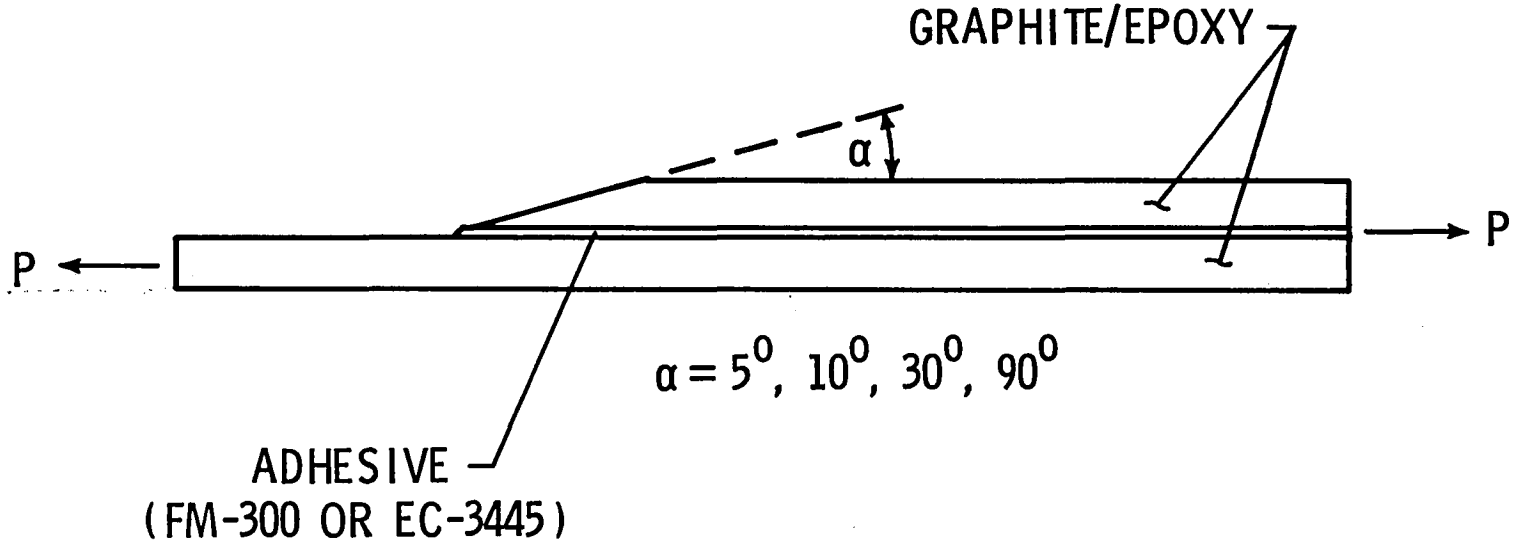

Figure 3.- Tapered cracked-lap-shear specimen.

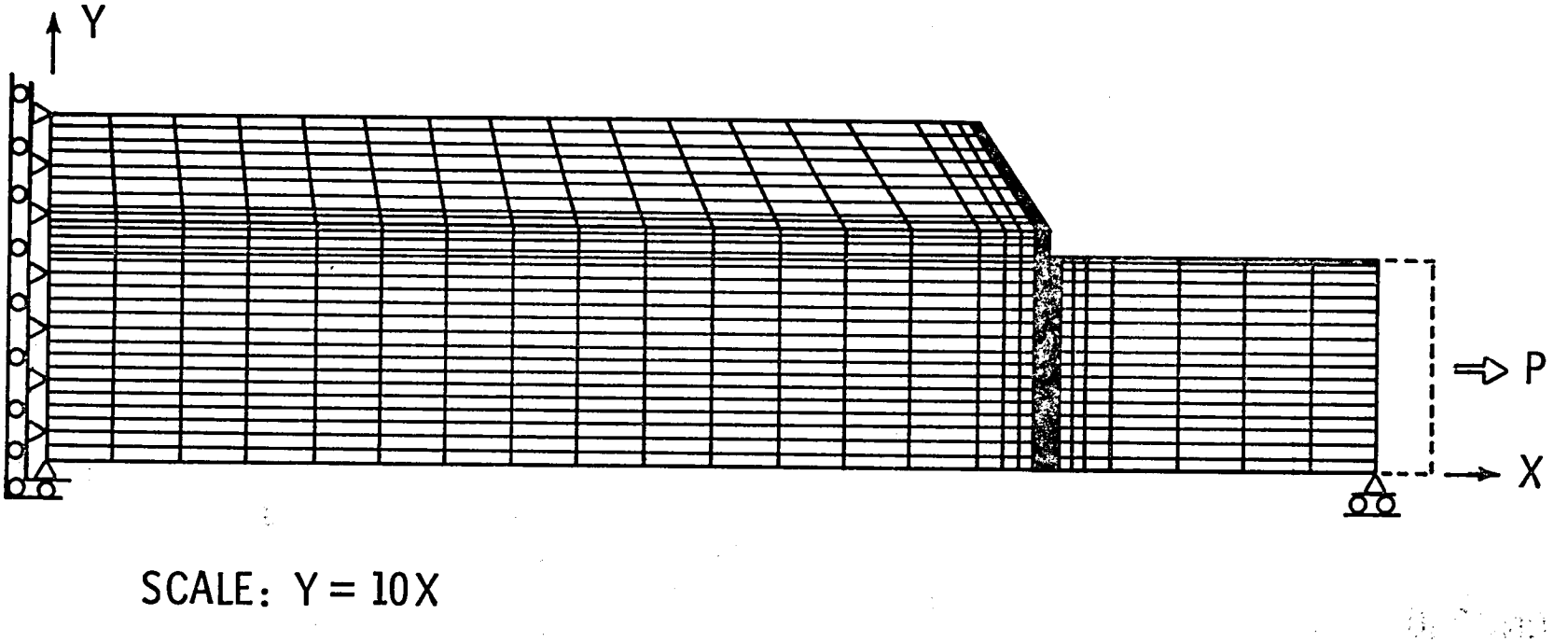

Figure 4.- Finite-element mesh of 10° tapered cracked-lap-shear specimen.

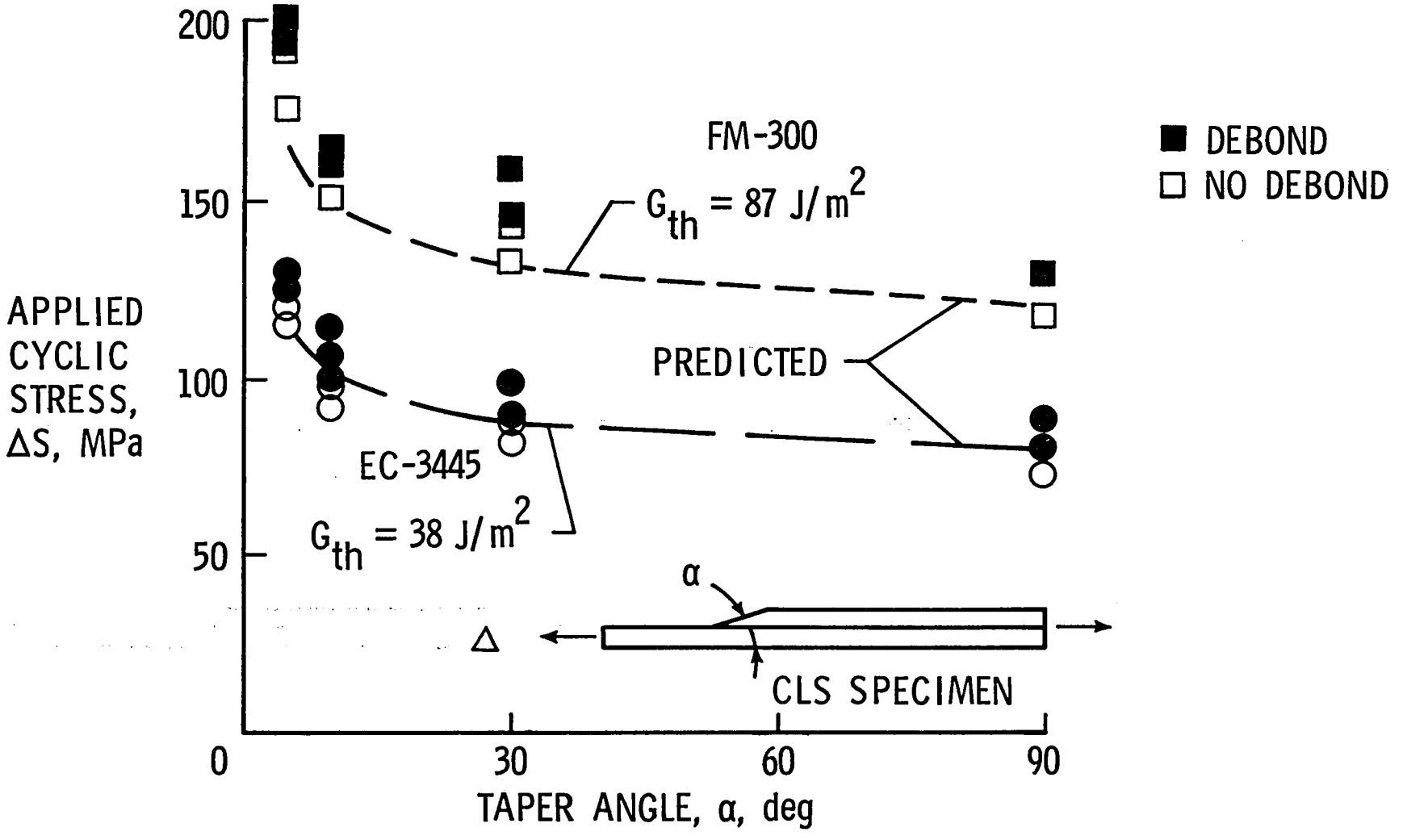

Figure 5.- Comparison of the predicted maximum stress for no debonding to experimental data.

1. Report No.	2. Government Accession No.	3. Recipient's Catalog No.
NASA TM-85694		

4. Title and Subtitle	5. Report Date
A FRACTURE MECHANICS APPROACH FOR DESIGNING ADHESIVELY BONDED JOINTS	September 1983
	6. Performing Organization Code 505-33-33-05
7. Author(s)	8. Performing Organization Report No.
W. S. Johnson and *S. Mall	
9. Performing Organization Name and Address	10. Work Unit No.
NASA Langley Research Center Hampton, VA 23665	11. Contract or Grant No.
	13. Type of Report and Period Covered Technical Memorandum
12. Sponsoring Agency Name and Address	14. Sponsoring Agency Code
National Aeronautics and Space Administration Washington, DC 20546	

15. Supplementary Notes *University of Maine, Orono, Maine.

To be presented at the ASTM Symposium on Delamination and Debonding of Materials, Philadelphia, Pennsylvania, November 8-10, 1983.

16. Abstract

An analytical and experimental investigation was undertaken to determine if the adhesive debond initiation stress could be predicted for arbitrary joint geometries. The analysis was based upon a threshold total strain-energy-release rate (G_{th}) concept. Two bonded systems were tested: T300/5208 graphite/epoxy adherends bonded with either EC-3445 or FM-300 adhesive. The G_{th} for each adhesive was determined from cracked-lap-shear (CLS) specimens by debond initiation tests. Finite-element analyses of various tapered CLS specimen geometries predicted the specimen stress at which the total strain-energy-release rate (G_T) equaled G_{th} at the joint tip. Experiments verified the predictions. The approach described herein predicts the maximum stress at which an adhesive joint can be cycled yet not debond. Furthermore, total strain-energy-release rate appeared to be the driving parameter for cyclic debonding and debond initiation in structural adhesives. In addition, debond initiation and growth were found to occur with virtually no peel stress present.

17. Key Words (Suggested by Author(s))	18. Distribution Statement
Adhesive joints Design Debond propagation Strain-energy-release rate Fracture mechanics	Unclassified - Unlimited Subject Category 39

19. Security Classif. (of this report)	20. Security Classif. (of this page)	21. No. of Pages	22. Price
Unclassified	Unclassified	21	A02

For sale by the National Technical Information Service, Springfield, Virginia 22161